Heliyon 10 (2024) e27247

Contents lists available at ScienceDirect

Heliyon

journal homepage: www.cell.com/heliyon

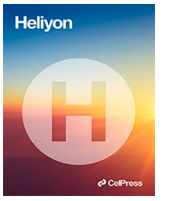

Research article

Bi doped LaOCl and LaOF thin films grown by pulsed laser deposition

Babiker M. Jaffar [a,b], H.C. Swart [a], H.A.A. Seed Ahmed [b], A. Yousif [b], R.E. Kroon [a,*]

[a] Department of Physics, Box 339, University of the Free State, Bloemfontein, 9300, South Africa
[b] Department of Physics, Box 321, University of Khartoum, Omdurman, 11115, Sudan

ARTICLE INFO

Keywords:
LaOCl
LaOF
Bismuth ions
Thin films
Pulsed laser deposition
Photoluminescence

ABSTRACT

Thin films of Bi^{3+} doped LaOCl and LaOF phosphors prepared via the pulsed laser deposition (PLD) technique in vacuum and different argon (Ar) pressures were compared in order to assess their luminescence properties. All peaks of the X-ray diffraction patterns of the films were consistent with the tetragonal structure of the LaOCl and LaOF, but in the case of LaOF the signal was weaker and not all peaks were present, suggesting some preferred orientation. Photoluminescence measurements revealed that the films exhibited emission around 344 nm for LaOCl:Bi and 518 nm for LaOF:Bi under excitations of 266 nm and 263 nm, respectively. The luminescence from the LaOF:Bi sample was less intense compared to the LaOCl:Bi sample prepared under the same conditions, which was also the case for the powder samples. The amount of ablated material present on the substrate was much less for LaOF:Bi compared to LaOCl:Bi, which is attributed to the greater bandgap and hence weaker absorption of the laser pulses for LaOF:Bi. Therefore phosphors based on LaOCl as the host material were found to be preferable over LaOF under the PLD conditions used in this study.

1. Introduction

The activated lanthanide oxyhalides (LnOX: Ln = La, Y, Gd and X = Cl, F, Br) are of interest because of their use as X-ray intensifying phosphors and they also have potential applications in fluoroscopic screens, cathode ray tubes and lamps. In particular, lanthanum oxyhalides (LaOX) have found much interest from researchers because of their excellent and unique magnetic, optical, electrical and luminescent characteristics [1,2]. Phosphor powders of LaOCl and LaOF doped with Bi have shown potential as stable phosphor materials. Although both these compounds have the same tetragonal PbFCl-type crystal structure with space group *P4/nmm* (No. 129) [3,4], Fig. 1 shows that the environment of the La^{3+} ion is different despite the same C_{4v} site symmetry in both cases. In LaOCl there is a Cl^- ion directly below each La^{3+} ion along the direction of the four-fold rotation axis and the Cl^- anions form double layers, whereas in LaOF the F^- ions are relatively rotated so as to be directly below the O^{2-} ions and form only single layers.

The luminescence properties of Bi^{3+} ions in a variety of host materials have been investigated widely [7]. The ground state of the Bi^{3+} ion is $^1S_0$, while the excited configuration consists of four energy levels, namely $^3P_0$, $^3P_1$, $^3P_2$ and $^1P_1$. The optical transition from $^1S_0$ to $^1P_1$ (C-band) is a spin allowed transition. The transition from $^1S_0$ to $^3P_1$ (A-band) is allowed because of the mixing of the $^1P_1$ and $^3P_1$ levels by spin-orbit coupling. The transition from $^1S_0$ to $^3P_2$ (B-band) is forbidden, but can be possible by coupling with unsymmetrical lattice vibrational modes. The transition from $^1S_0$ to $^3P_0$ is strongly forbidden [8]. Bi^{3+} ions substitute La^{3+} ions in doped

* Corresponding author.
E-mail address: KroonRE@ufs.ac.za (R.E. Kroon).

https://doi.org/10.1016/j.heliyon.2024.e27247
Received 23 November 2023; Received in revised form 8 February 2024; Accepted 27 February 2024
Available online 28 February 2024

samples (due to their similar ionic radii and equal valence) and the difference in environment has a strong effect on the Bi^{3+} luminescence. While LaOCl:Bi powder emits in the ultraviolet, the emission of LaOF:Bi powder is strongly red-shifted into the visible range with much greater Stokes shift.

Thin film phosphors have significant advantages compared to common powder forms, e.g. relatively large thermal stability, structural density, better coherence with the basic substrates and effective thermal dissipation for high energy operation [9]. Pulsed laser deposition (PLD) has been commonly used for the preparation of thin films of a wide number of materials [10–12]. PLD is a relatively new technique for depositing thin films using high energy laser pulses to evaporate the surface of the material target inside a vacuum chamber and condensing the vapour on the surface of a substrate to create a thin film layer with a thickness of up to a few micrometres [13]. Thin films that have been produced using PLD can be applied in devices for a number of technologies, including environmental sensors, micromechanical devices, light emitters, electron emitters, medical implants, and various coatings [11]. Despite phosphors generally being produced commercially as powders, thin films are important in most commercial applications where films of uniform thickness on large-area substrates are of interest, and PLD is widely used in research laboratories for the growth of thin luminescent films because of the conceptual simplicity of the process [10]. The PLD technique has a high ability to control the formation of thin films, morphology, composition and growth process by varying the partial pressure of a gas in the deposition chamber and selecting the substrate temperature [14]. As a result of the multiple processes involved, such as laser absorption, plume formation, and film growth, the PLD approach is exceedingly complicated and this is exacerbated at high pressures, yielding a diverse array of nanostructures with variable stoichiometric and size distributions [10].

Thin films of LaOCl formed by evaporation of LaB_6 on NaCl [15] and sol-gel LaOF [16] have been studied some time ago. In this novel work, thin films of Bi^{3+} doped LaOCl and LaOF phosphors prepared via the pulsed laser deposition (PLD) technique in vacuum and different argon (Ar) pressures were compared in order to assess their luminescence properties. The aim of this work is to investigate the properties of LaOX (X = Cl, F) crystalline thin films doped with Bi prepared by using the PLD technique in a vacuum and different argon (Ar) pressures. Ar was selected since it is a non-reactive gas, rather than oxygen which may have unintentionally oxidized the oxyhalide materials during deposition. The influence of the pressure of the background Ar atmosphere on the structural and optical properties of the thin films was studied, while keeping other experimental parameters such as substrate temperature, target to substrate distance and deposition times constant. In the following sections, we first present the experimental procedure, then provide information on the structure and morphology of the thin films, and finally assess their luminescence properties.

2. Experimental

To create a target for the laser ablation, powder samples of $La_{1-x}OCl:Bi_x$ and $La_{1-x}OF:Bi_x$ were first prepared via the solid-state reaction method. For the oxychloride the optimum synthesis temperature was 900 °C with doping concentration x = 0.007 [17], while for the oxyfluoride the corresponding values were 1000 °C and x = 0.005 [18]. These powders were pressed using a hydraulic press to make target pellets which were annealed at 900 °C for 8 h in air to remove all adventitious water containing species that may be present and then transferred to the chamber of the PLD system and positioned on a rotating target holder. Annealing of the target pellets was found to be vital to prevent them from breaking apart to emit a powder of the material inside the PLD deposition chamber under the action of the laser.

Si (100) substrates were cleaned in an ultrasonic bath using acetone, ethanol and finally distilled water bath consecutively for 15 min each. The cleaned substrates were then dry blown with nitrogen gas. The PLD system was pumped to a base pressure of 5 x 10^{-5} mbar (~0.04 mTorr) and a thin film was deposited under these conditions (referred to as 'vacuum'). Additional films were created in a similar way, except that the deposition chamber was pumped to base pressure and then back-filled with Ar to a pressure of 10, 20 or 40 mTorr. A frequency quadrupled Nd:YAG pulsed laser emitting at 266 nm was used to ablate the targets. The laser energy (40 mJ/

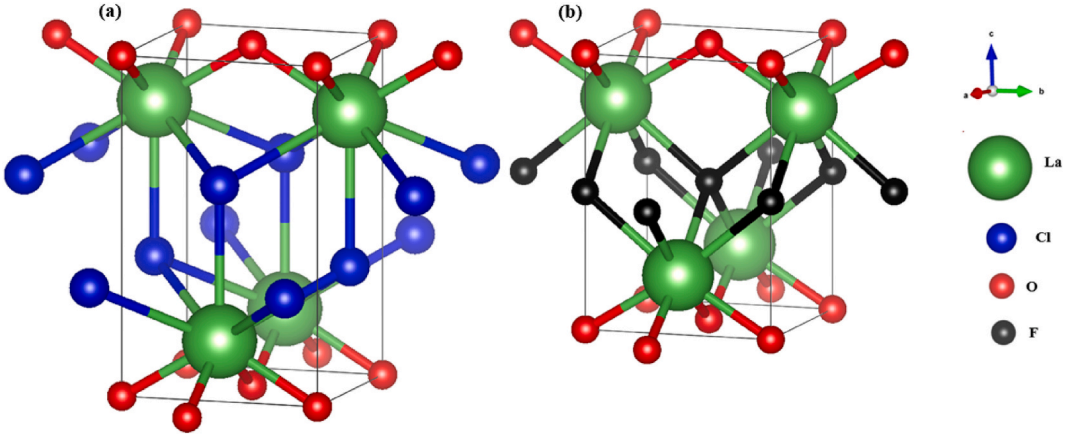

Fig. 1. The unit cell of (a) LaOCl and (b) LaOF modelled with Vesta software [5] using CIF files obtained from the Crystallography Open Database [6], number 1539093 for LaOCl and number 7037053 for LaOF.

pulse), fluency and target-to-substrate distance fixed at 30 Hz, 1.7 J/cm^2 and 4.5 cm, respectively. The deposition time was 20 min and the substrate temperature was fixed at 300 °C.

The crystal structures were assessed using X-ray diffraction (XRD) measurements made with a Bruker D8 Advance diffractometer. To produce the Cu Kα characteristic X-rays used, an electron beam of current 40 mA was accelerated through 40 kV and scans were made in steps of 0.02° with a scan rate of 1 s per step. The samples were examined using a JEOL JSM-7800F scanning electron microscope (SEM) operating at 5 keV and the elemental composition was assessed by means of its energy dispersive X-ray spectroscopy (EDS) attachment (X-Max^{N}80 detector) by Oxford Instruments with an electron beam of 10 kV. The PL properties of the films were measured at room temperature using an FLS980 spectrometer from Edinburgh Instruments with a continuous 450 W xenon lamp and double excitation and emission monochromators.

3. Results and discussion

3.1. Structure, morphology and chemical composition analysis

Fig. 2 shows the XRD patterns of (a) LaOCl:Bi and (b) LaOF:Bi thin films deposited in vacuum and different Ar pressures, together with the powders that were used to make the PLD targets. For the LaOCl:Bi shown in Fig. 2(a) all peak positions matched well with the corresponding powder, which has previously been matched to record PDF #080477 of LaOCl [17]. The XRD signal from the LaOF:Bi thin films was comparatively weaker, as can be seen by the greater relative signal-to-noise ratio in Fig. 2(b). The thin film of LaOF:Bi produced in vacuum displayed the three most intense peaks corresponding to the powder, which has previously been matched to record PDF #080477 of LaOF [18]. For the other samples created in Ar environments, the diffraction peak at 26.7° dominated the XRD patterns, indicating some preferential orientation of the (101) plane. As the Ar gas pressure increased, the intensity of the 101 diffraction peak increased, suggesting an increase in the thicknesses of the films. The sample grown in 10 mTorr Ar also displayed several sharp additional diffraction peaks (marked with asterisks, *). These peaks were also found for a clean substrate having no deposited film and are due to the weak (forbidden) Si 200 peak near 33° and also some Si 400 peaks for weak X-rays of different wavelengths due to tungsten (W) contamination of the Cu anode [19].

The average crystallite sizes for the LaOCl:Bi and LaOF:Bi thin films were determined using the Scherrer equation [20], $D = \frac{0.9\lambda}{\beta \cos\theta}$, where λ is the X-ray wavelength and θ is the Bragg angle. The crystallite size may be used as an indication of the crystallinity. The results are tabulated in Table 1 and show that the average crystallite size for the LaOCl:Bi for the film deposited in a vacuum is smaller than those deposited in different Ar pressures and the average crystallite size increased with increasing Ar pressure. The opposite trend was obtained for LaOF:Bi where the average crystallite size of the film deposited in a vacuum is greater than those deposited in

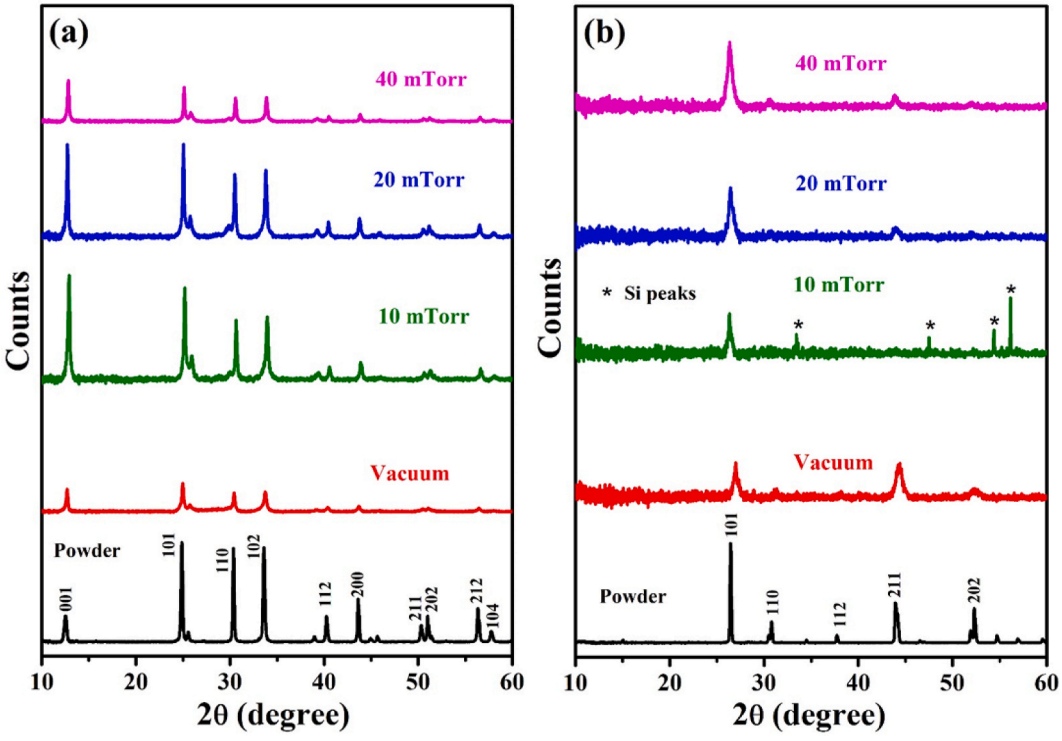

Fig. 2. XRD patterns of (a) LaOCl:Bi and (b) LaOF:Bi thin films deposited in vacuum and different Ar pressures, compared to the powders from which PLD target was made. The powders match the standards PDF #080477 for LaOCl [17] and #080477 of LaOF [18] reported previously.

Table 1
Crystallite sizes (nm) calculated from the Scherrer equation.

Film	Base pressure ~0.04 mTorr	Ar gas pressure		
		10 mTorr	20 mTorr	40 mTorr
LaOCl:Bi	27	32	34	36
LaOF:Bi	20	18	16	12

different Ar pressures and decreased with increasing Ar pressure. This indicates that LaOCl and LaOF do not perform similarly during laser ablation and PLD. Therefore other factors in addition to the Ar pressure must be significant in determining the crystallinity of the thin films. We discuss this further after presenting the PL results in section 3.3.

Fig. 3 presents the plan-view and cross-sectional SEM images and EDS spectra of the LaOCl:Bi thin films. The images show that the particles had different spherical sizes for the film deposited in a vacuum. The films deposited in different Ar pressures had particles of different spherical sizes as well as flower-like shapes with platelets. The cross-sectional images of the thin films were similar and clearly revealed the presence of spherical particles and flower-like shapes in the morphology. The roughness of the film indicated that a significant portion of the material arrived at the substrate in the form of particulates rather than atoms. While such particulates are undesirable in many applications, a smooth film can inhibit emission of luminescence out of the layer normal to the surface (due to internal reflections) and increasing the surface roughness is generally beneficial [21]. Particulates deposited on the substrate during

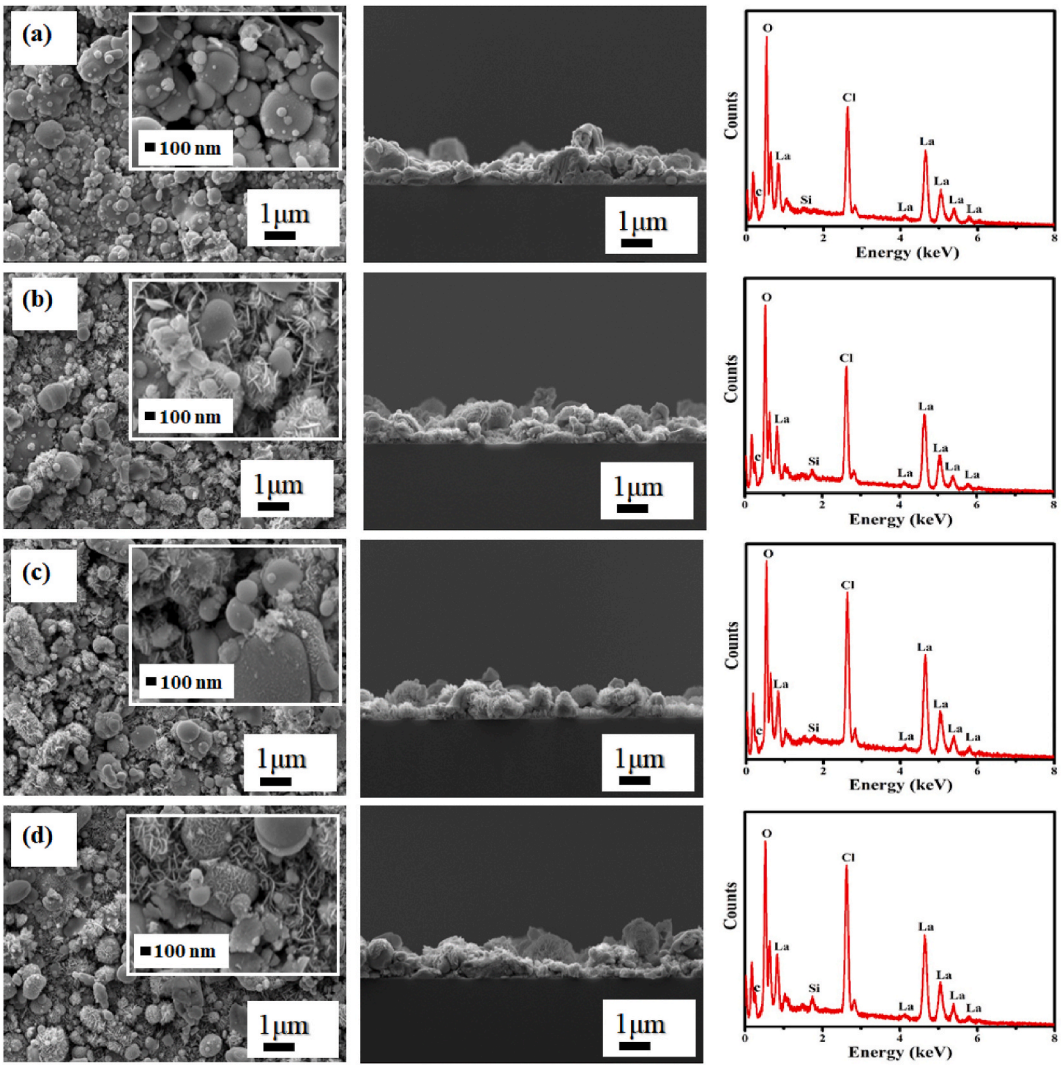

Fig. 3. Plan view and cross sectional SEM images as well as EDS (over the region shown in the plan view) of LaOCl:Bi thin films deposited (a) in vacuum and with different Ar pressures of (b) 10, (c) 20 and (d) 40 mTorr.

PLD can, in general, originate from material ejected from the target in solid, liquid or vapour state. Molten material generally forms particulates in the micrometer range with rounded or spherical features [22] as observed for the large particulates in the inset of Fig. 3 (a). In this study the substrate temperature was fixed at 300 °C, but increasing the substrate temperature during PLD deposition of Y_2O_3:Ho,Yb phosphor [23] was shown to significantly reduce the surface roughness of the film, so additional work varying the substrate temperature may be beneficial in future. The EDS spectra of the films are similar to the powders, indicating good transfer of stoichiometry from the target to thin film during PLD. Although it has been reported that the background gas may cause preferential scattering of lighter elements in the plume so that these elements may be deficient in the ablated film [24], and this effect should increase with increasing background gas pressure, in this work the relative size of the EDS peaks corresponding to different elements was not found to vary, i.e. changing the Ar pressure did not affect the chemical composition of the films. This, and the similar thicknesses of the LaOCl:Bi films, indicate that the varying Ar gas pressure did not have a strong influence on the PLD growth process for this material. The presence of Si in the EDS spectra was due to the Si substrate.

Fig. 4 presents the plan-view and cross-sectional SEM images and EDS spectra of LaOF:Bi thin films. Note that the magnification is greater than in Fig. 3 for LaOCl. Particles of spherical shape with distinct sizes were observed. The cross-sectional images were similar and confirmed the presence of spherical particles in the morphology, which are particulates from the ejection of molten material from the target [22]. It is clear from the SEM images that the films consisted of much less material than for the corresponding films of LaOCl. The EDS spectra of the films are similar to the powder, indicating that the stoichiometry is retained from the target to thin film during PLD. The EDS spectra of the thin films also show the Si peak from the substrate. This is much more prominent for the films of LaOF than for the films of LaOCl and the Si peak dominates the EDS spectrum of the LaOF film deposited at an Ar pressure of 10 mTorr, which also showed XRD peaks due to the Si substrate (Fig. 2(b)). The relative size of the Si EDS peak decreased for the LaOF films grown at higher

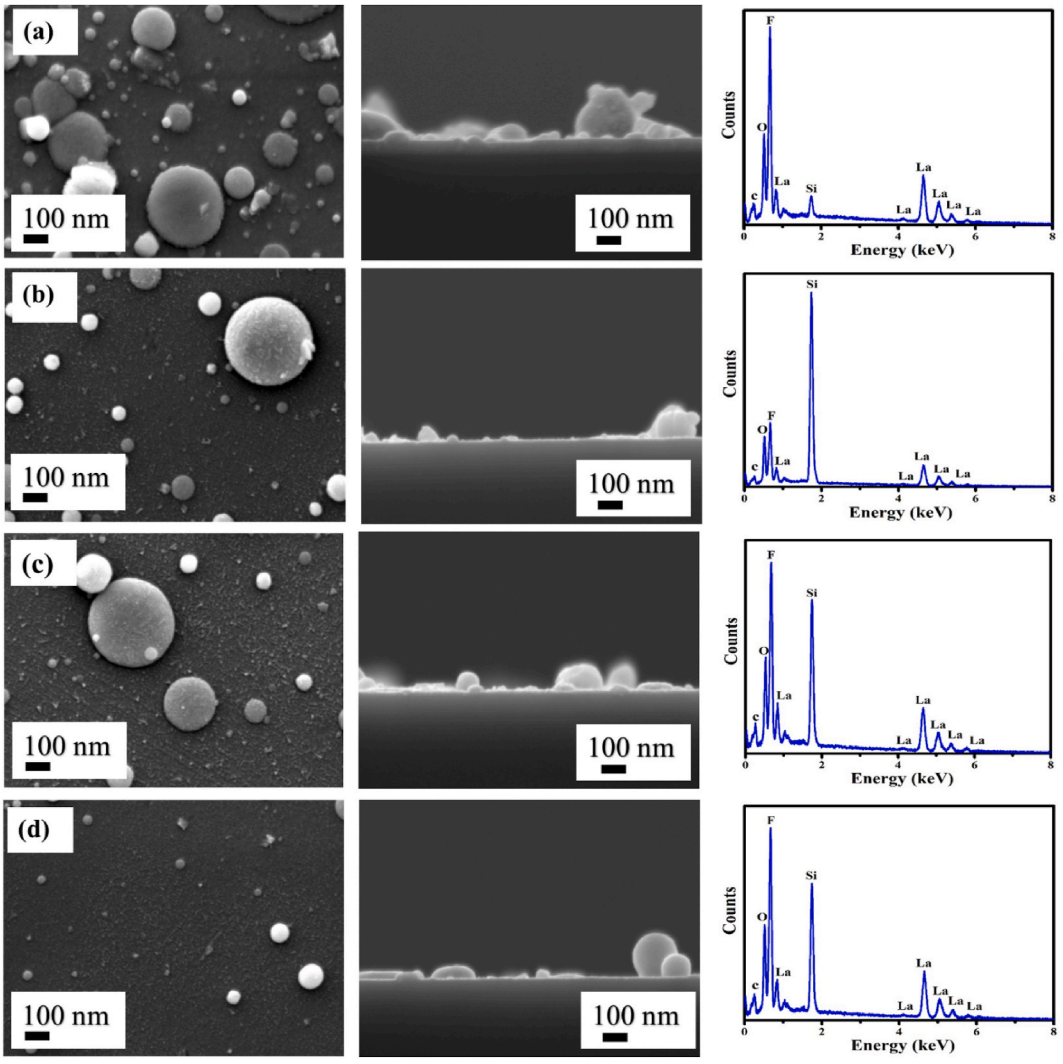

Fig. 4. Plan view and cross sectional SEM images as well as EDS (over the region shown in the plan view) of LaOF:Bi thin films deposited (a) in vacuum and with different Ar pressures of (b) 10, (c) 20 and (d) 40 mTorr.

Ar pressures of 20 and 40 mTorr, but these films still consist of very little material. The thickest LaOF film, which can be observed for the cross-sectional SEM image and has the smallest Si EDS peak, was created under vacuum PLD conditions. Therefore the presence of a background gas to reduce the kinetic energy of ablated material before reaching the substrate was not beneficial for the growth of LaOF films.

3.2. Photoluminescence analysis

Fig. 5(a and b) display the PL excitation and emission spectra of the LaOCl:Bi and LaOF:Bi powder samples with emission bands at around 344 nm and at 518 nm under excitations of 266 nm and 263 nm, respectively. These excitation and emission peaks have been attributed to the transitions between the $^3P_1$ excited state and $^1S_0$ ground state of the Bi^{3+} ions. Fig. 5(c and d) show the PL excitation and emission spectra of the thin films. The energy level diagrams for Bi^{3+} in these two hosts (Fig. 6) is similar to that in La_2O_3 [25]. The Stokes shift in the LaOF host is significantly greater than for LaOCl, indicating that the excited level minima are more strongly offset from the ground state minimum for LaOF, as a result of the different environments of Bi^{3+} ions which are substituting the La^{3+} ions shown in Fig. 1.

While the form of the PL emission of the LaOCl and LaOF:Bi thin films matched that of the powders, the films deposited in vacuum for both compounds showed the lowest intensity. This is unexpected for the LaOF:Bi films since for this material the film grown in vacuum was the thickest. For the LaOCl:Bi thin films deposited in Ar the PL emission intensity increased with increasing Ar gas pressures, while the PL intensity for the LaOF:Bi thin films deposited in Ar increased with the increase of the Ar gas pressures up to 20 mTorr and then decreased with a further increase in Ar gas pressure. However, the emission of LaOF:Bi deposited in vacuum showed a shoulder peak at around 380 nm, which may originate from defect emission. This emission has been attributed to individual ionizing oxygen vacancies in LaOF, which results from the recombination of a photogenerated hole with an electron occupying an oxygen vacancy [26,27]. The presence of a high concentration of such defects in the LaOF:Bi film formed in vacuum could increase non-radiative recombination pathways for excited Bi^{3+} ions and quench their luminescence.

Fig. 7(a) displays the PL emission spectra of the LaOCl:Bi and LaOF:Bi powder samples, which are compared in Fig. 7(b) to the

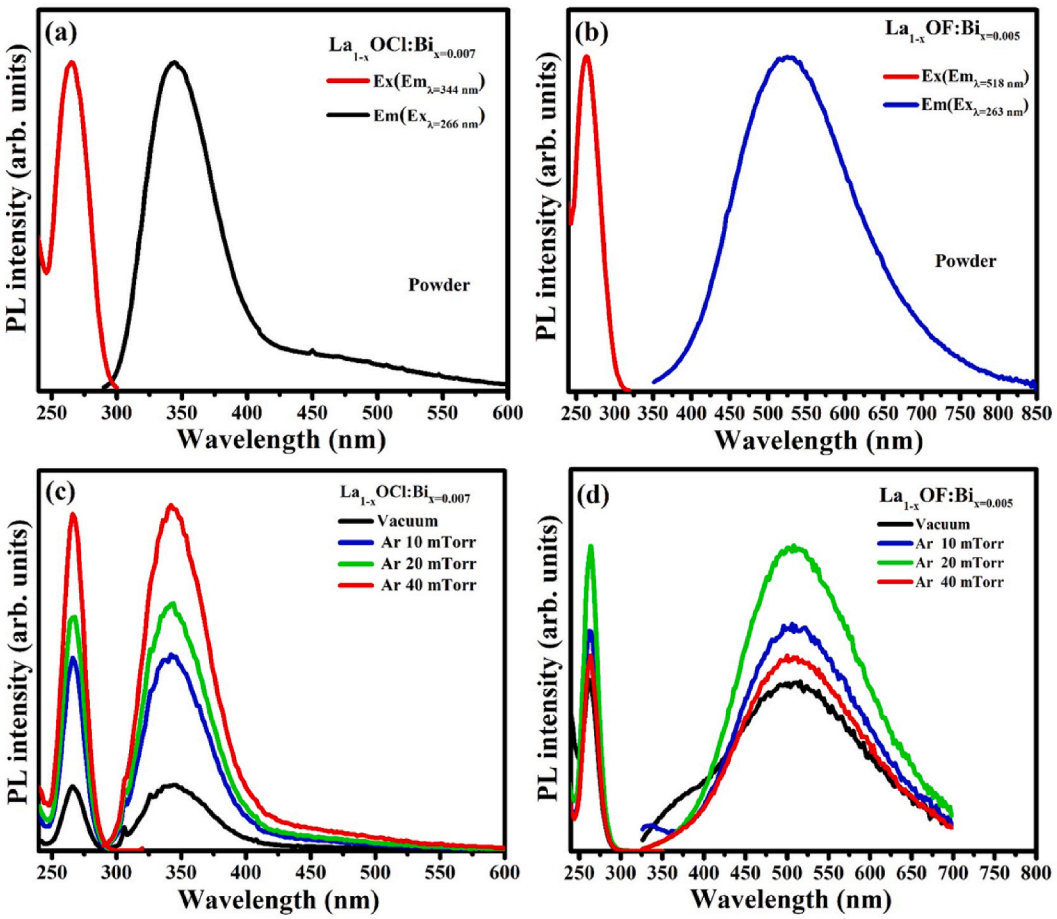

Fig. 5. PL excitation and emission spectra of the $La_{1-x}OCl:Bi_{x\,=\,0.007}$ and $La_{1-x}OF:Bi_{x\,=\,0.005}$ (a, b) for the powders and (c, d) PLD thin films deposited in vacuum and different Ar pressures, respectively.

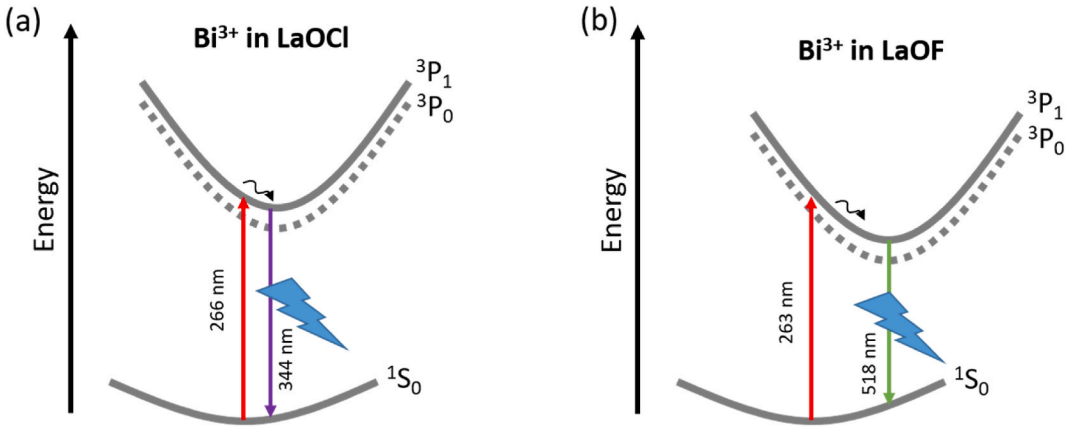

Fig. 6. Energy level diagrams for Bi^{3+} ions in (a) LaOCl:Bi with small Stokes shift and (b) LaOF:Bi with large Stokes shift.

intensities and wavelengths of the emission for the best LaOCl:Bi and LaOF:Bi thin films, produced under Ar pressures of thin film 40 and 20 mTorr, respectively. The emission spectra of the LaOCl:Bi powder and film was narrow and at shorter wavelength than the corresponding emission spectra of LaOF:Bi. For both powder and films, the luminescence from the LaOF:Bi samples was less intense compared to the corresponding LaOCl:Bi samples.

While PLD worked well to produce thin films of LaOCl:Bi, the quality of the LaOF:Bi films which were created was less good. The layers were much thinner and less material was deposited. A reason for this may be the different bandgaps of LaOCl and LaOF. We determined the band gap of LaOCl powder to be 5.76 eV (~215 nm). The bandgap of LaOF was difficult to measure with our instrument, which only measures down to 200 nm, but is expected to be greater than that of LaOCl since the bandgap of LnOX increases as X varies from I to Br to Cl to F [28,29]. In both cases the bandgap of the materials is greater than the energy corresponding to the 266 nm PLD laser photons which will limit strong absorption. Since the bandgap of LaOF is bigger than that of LaOCl, it will absorb the PLD laser light even less effectively and therefore the laser pulse energy will be spread through a greater volume, so the material is less heated and not as much is ablated. This indicates that the PLD laser wavelength, relative to the bandgap of the target material, can have a strong influence on the quality of thin films produced by PLD. This challenge has also been recently noted in a tutorial review on pulsed laser deposition, where some large bandgap oxides such as MgO, Al_2O_3 and SiO_2 were identified as challenging to ablate with the commonly used 248 nm KrF excimer laser [30].

4. Conclusion

Bi doped LaOCl and LaOF phosphor thin films were successfully synthesized by the PLD technique. XRD data confirmed that both LaOCl and LaOF phases belong to the tetragonal crystal structure. The SEM images of LaOCl show that the particles had different spherical sizes for the film deposited in a vacuum. The films deposited in different Ar pressures had particles of different spherical sizes as well as flower-like shapes with platelets. The SEM images of LaOF show that the particles had spherical shape with distinct sizes. The LaOF films consisted of much less material than for the corresponding films of LaOCl. The EDS spectra of the films are similar to the powder. Photoluminescence measurements revealed that the films exhibited emission around 344 nm for LaOCl:Bi and 518 nm for LaOF:Bi under excitations of 266 nm and 263 nm, respectively. These excitation and emission peaks have been attributed to the transitions between the $^3P_1$ excited state and $^1S_0$ ground state of the Bi^{3+} ions. For both powder and films, the luminescence from the LaOF:Bi samples was less intense compared to the corresponding LaOCl:Bi samples. In future work the porosity and roughness of the LaOCl:Bi films may be investigated with varying substrate temperature, while a shorter wavelength or shorter pulse excitation laser would improve the ablation of the very large bandgap LaOF:Bi material.

CRediT authorship contribution statement

Babiker M. Jaffar: Writing – original draft, Investigation, Conceptualization. **H.C. Swart:** Writing – review & editing, Supervision, Resources, Funding acquisition. **H.A.A. Seed Ahmed:** Writing – review & editing, Supervision. **A. Yousif:** Writing – review & editing, Supervision. **R.E. Kroon:** Writing – review & editing, Supervision, Resources, Methodology, Investigation, Funding acquisition, Conceptualization.

Declaration of competing interest

The authors declare that they have no known competing financial interests or personal relationships that could have appeared to influence the work reported in this paper.

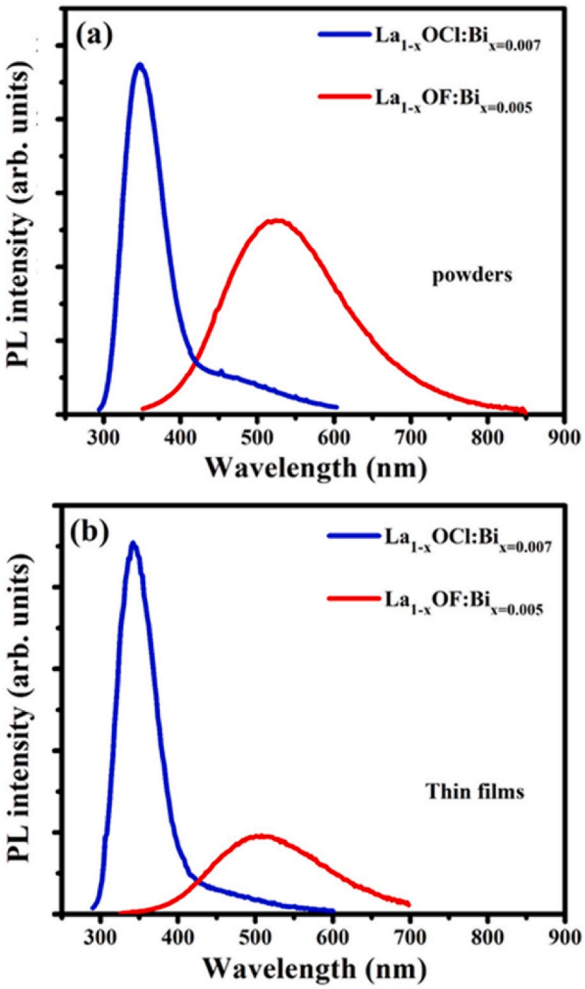

Fig. 7. PL emission spectra of LaOCl:Bi and LaOF:Bi (a) powders and (b) PLD thin films deposited in Ar pressure showing the strongest emission.

Acknowledgements

This work is based on the research supported by the South Africa research chair initiative of the Department of Science and Technology (84415). The first author was financially supported by the African Laser Centre. National Research Foundation of South Africa (Grant no. 93214, R.E. Kroon) for photoluminescence measurements.

References

[1] G. Shwetha, V. Kanchana, N. Yedukondalu, G. Vaitheeswaran, Ab initio study of scintillating lanthanide oxyhalide host materials, Mater. Res. Express 2 (2015) 105901, https://doi.org/10.1088/2053-1591/2/10/105901.

[2] U. Rambabu, A. Mathur, S. Buddhudu, Fluorescence spectra of Eu^{+3} and Tb^{+3}-doped lanthanide oxychloride powder phosphors, Mater. Chem. Phys. 61 (1999) 156–162, https://doi.org/10.1016/s0254-0584(99)00122-4.

[3] Kenneth R. Kort, Sarbajit Banerjee, Shape-controlled synthesis of well-defined matlockite LnOCl (Ln: La, Ce, Gd, Dy) nanocrystals by a novel non-hydrolytic approach, J. Inorg. Chem. 50 (2011) 5539–5544, https://doi.org/10.1021/ic200114s.

[4] J.W. Fergus, Crystal structure of lanthanum oxyfluoride, J. Mater. Sci. Lett. 16 (1997) 267–269, https://doi.org/10.1023/A:1018584614532.

[5] Koichi Momma, Fujio Izumi, VESTA 3 for three-dimensional Visualization of crystal, Volumetric and morphology data, J. Appl. Crystallogr. 44 (2011) 1272–1276, https://doi.org/10.1107/S0021889811038970.

[6] A. Vaitkus, A. Merkys, S. Gražulis, Validation of the Crystallography open Database using the Crystallographic information framework, J. Appl. Crystallogr. 54 (2021) 661–672, https://doi.org/10.1107/S1600576720016532.

[7] Roy H.P. Awater, Pieter Dorenbos, The Bi^{3+} 6s and 6p electron binding energies in relation to the chemical environment of inorganic compounds, J. Lumin. 184 (2017) 221–231, https://doi.org/10.1016/j.jlumin.2016.12.021.

[8] A.M. Srivastava, S.J. Camardello, Concentration dependence of the Bi^{3+} luminescence in $LnPO_4$ (Ln = Y^{3+}, Lu^{3+}), Opt. Mater. 39 (2015) 130–133, https://doi.org/10.1016/j.optmat.2014.11.011.

[9] A. Yousif, H.C. Swart, O.M. Ntwaeaborwa, E. Coetsee, Conversion of $Y_3(Al,Ga)_5O_{12}:Tb^{3+}$ to $Y_2Si_2O_7:Tb^{3+}$ thin film by annealing at higher temperatures, Appl. Surf. Sci. 270 (2013) 331–339, https://doi.org/10.1016/j.apsusc.2013.01.025.

[10] Adawiya J. Haider, Taif Alawsi, Mohammed J. Haider, Bakr Ahmed Taha, Haydar Abdulameer Marhoon, A comprehensive review on pulsed laser deposition technique to effective nanostructure production: trends and challenges, Opt. Quant. Electron. 54 (2022) 488, https://doi.org/10.1007/s11082-022-03786-6.

[11] Khalid Bin Masood, Pushpendra Kumar, Mushtaq Ahmad Malik, Jai Singh, A comprehensive tutorial on the pulsed laser deposition technique and developments in the fabrication of low dimensional systems and nanostructures, Emergent Materials 4 (2021) 737–754, https://doi.org/10.1007/s42247-020-00155-5.
[12] Simon N. Ogugua, Odireleng Martin Ntwaeaborwa, Hendrik C. Swart, Latest development on pulsed laser deposited thin films for advanced luminescence applications, Coatings 10 (2020) 1078, https://doi.org/10.3390/coatings10111078.
[13] Z. Liu, Laser Applied Coatings, Shreir's Corrosion, 2010, pp. 2622–2635, https://doi.org/10.1016/B978-044452787-5.00141-4.
[14] R.M. Jafer, H.C. Swart, A. Yousif, E. Coetsee, The effect of different substrate temperatures on the structure and luminescence properties of Y_2O_3:Bi^{3+} thin films, Solid State Science 53 (2016) 30–36, https://doi.org/10.1016/j.solidstatesciences.2016.01.005.
[15] Shigeo Horiuchi, Chuhei Oshima, Growth of LaOCl crystalline films, J. Cryst. Growth 23 (1974) 239–241, https://doi.org/10.1016/0022-0248(74)90243-7.
[16] S. Fujihara, T. Kato, T. Kimura, Sol-gel synthesis and luminescent properties of oxyfluoride LaOF:Eu^{3+} thin films, Materials Science Letters 20 (2001) 687–689, https://doi.org/10.1023/a:1010946621624.
[17] Babiker M. Jaffar, H.C. Swart, H.A.A. Seed Ahmed, A. Yousif, R.E. Kroon, Comparative study of the luminescence of Bi doped LaOCl and LaOBr phosphor powders, J. Lumin. 250 (2022) 119050, https://doi.org/10.1016/j.jlumin.2022.119050.
[18] Babiker M. Jaffar, H.C. Swart, H.A.A. Seed Ahmed, A. Yousif, R.E. Kroon, Luminescence properties of Bi doped LaOF phosphor powder, Opt. Mater. 135 (2023) 113367, https://doi.org/10.1016/j.optmat.2022.113367.
[19] E.H.H. Hasabeldaim, O.M. Ntwaeaborwa, R.E. Kroon, E. Coetsee-Hugo, H.C. Swart, Pulsed laser deposition of a ZnO:Eu^{3+} thin film: study of the luminescence and surface state under electron beam irradiation, Appl. Surf. Sci. (2019) 144281, https://doi.org/10.1016/j.apsusc.2019.144281.
[20] R.E. TedKroon, Nanoscience and the scherrer equation versus the 'scherrer–gottingen equation', South Afr. J. Sci. 109 (5/6) (2013) https://doi.org/10.1590/sajs.2013/a0019. Art. #a0019 (2 pages).
[21] R.K. Singh, Z. Chen, D. Kumar, K. Cho, M. Ollinger, Critical issues in enhancing brightness in thin film phosphors for flat-panel display applications, Appl. Surf. Sci. 197–198 (2002) 321–324, https://doi.org/10.1016/S0169-4332(02)00390-2.
[22] L. Chen, Particulates generated by pulsed laser ablation, in: D.B. Chrisey, G.K. Hubler (Eds.), Pulsed Laser Deposition of Thin Films, John Wiley and Sons, New York, 1994 (Chapter 5) in.
[23] Anurag Pandey, Vinod Kumar, R.E. Kroon, H.C. Swart, Temperature induced upconversion behaviour of Ho^{3+}-Yb^{3+} codoped yttrium oxide films prepared by pulsed laser deposition, J. Alloys Compd. 672 (2016) 190–196, https://doi.org/10.1016/j.jallcom.2016.02.131.
[24] C.N. Afonso, J. Gonzalo, Pulsed laser deposition of thin films for optical applications, Nucl. Instrum. Methods Phys. Res. B 116 (1996) 404–409, https://doi.org/10.1016/0168-583X(96)00078-X.
[25] B.M. Jaffar, H.C. Swart, H.A.A. Seed Ahmed, A. Yousif, R.E. Kroon, Luminescence properties of Bi doped La_2O_3 powder phosphor, J. Lumin. 209 (2019) 217–224, https://doi.org/10.1016/j.jlumin.2019.01.044.
[26] Guguloth Ravi, Madderla Sarasija, Dasari Ayodhya, Lunavath Shanthi Kumari, Dongamanti Ashok, Facile synthesis, characterization and enhanced catalytic reduction of 4-nitrophenol using $NaBH_4$ by undoped and Sm^{3+}, Gd^{3+}, Hf^{3+} doped La_2O_3 nanoparticles, Nano Convergence 6 (2019) 1–9, https://doi.org/10.1186/s40580-019-0181-6.
[27] Chenguo Hu, Hong Liu, Wenting Dong, Yiyi Zhang, Gang Bao, Changshi Lao, L. Zhong, Wang, La$(OH)_3$ and La_2O_3 nanobelts - synthesis and physical properties, Adv. Mater. 19 (2007) 470–474, https://doi.org/10.1002/adma.200601300.
[28] D. Kim, J.R. Jeong, Y. Jang, J.-S. Bae, I. Chung, R. Liang, J.-C. Park, Self-emitting blue and red EuOX (X = F, Cl, Br, I) materials: band structure, charge transfer energy, and emission energy, Phys. Chem. Chem. Phys. 21 (2019) 1737–1747, https://doi.org/10.1039/c8cp06470a.
[29] D. Kim, S. Park, S. Kim, S.-G. Kang, J.-C. Park, Blue-emitting Eu^{2+}-activated LaOX (X = Cl, Br, and I) materials: crystal field effect, Inorg. Chem. 53 (2014) 11966–11973, https://doi.org/10.1021/ic5015576.
[30] Nick A. Shepelin, Zahra P. Tehrani, Natacha Ohannessian, Christof W. Schneider, Daniele Pergolesi, Thomas Lippert, A practical guide to pulsed laser deposition, Chem. Soc. Rev. 52 (2023) 2294, https://doi.org/10.1039/d2cs00938b.